The VCI-P code: an iterative variation–perturbation scheme for efficient computations of anharmonic vibrational levels and IR intensities of polyatomic molecules

Philippe Carbonnière · Alain Dargelos · Claude Pouchan

Abstract A variation–perturbation scheme called VCI-P code is proposed. It is developed mainly for the efficient and accurate theoretical description of vibrational resonances in polyatomic molecules. This state-specific process consists of the iterative construction of small matrices for each vibrational state, using the most important configurations contributing to that state. The weak couplings are considered perturbationally. The keypoint of this paper is a recipe that allows the massive truncation of the vibrational configuration space with minimum error in the calculated energies. The anharmonic frequencies and IR/vibrational absorption (VA) intensities obtained using VCI-P for methane and formaldehyde are compared to their full VCI counterparts. The convergence of the VCI-P results with respect to configuration selection is also discussed from the examples of *trans*-difluoroethylene and ethylene oxide (also called oxirane). A parallelization scheme for the $3N - 5$ calculations on distributed memory computers is proposed. Representative computational times are presented for molecules ranging in size from 4 to 15 atoms.

Keywords Algorithm · Anharmonic vibrational level · Anharmonic intensity · Variation · Perturbation

P. Carbonnière (✉) · A. Dargelos · C. Pouchan
Groupe de Chimie Théorique et Réactivité,
IPREM/ECP UMR CNRS 5254,
Université de Pau et des Pays de l'Adour,
64000 Pau, France
e-mail: philippe.carbonniere@univ-pau.fr

1 Introduction

The accurate description of vibrational properties for large molecular systems is a very challenging exercise for several reasons. From an experimental point of view, vibrational spectroscopy is far from being a 'vanishing' discipline [1] due to the wide range of domains in which the vibrational fingerprint of molecular systems is needed for substance recognition/identification. In the field of chemistry, beside routine qualitative (functional group) and quantitative (concentration) analyses, applications such as structural and conformational analysis [2–4], molecular design [5, 6], and reactivity monitoring [7–9] can be based on the modeling of vibrational effects. Nevertheless, the band assignment of an experimental spectrum is not straightforward since multiple effects (such as, for instance, anharmonicity, presence of overtones and combinations bands, dynamic and environmental effects) play a relevant and intermingled role. From a theoretical point of view, the requirement to go beyond the harmonic approximation for a proper treatment of the vibrational properties (or vibrationally averaged properties [10, 11]) renders the problem non-trivial. It is undertaken using two different ways: the time-dependent approaches that consist of a vibrational analysis from molecular dynamics trajectories [12] and the so-called static methods based on a quantum mechanical/stationary-state picture of the system. In the first case, the standard statistical mechanics formalism relies on Fourier transform analysis of the time correlation of atomic velocities or dipole moment. In principle, these approaches can provide a complete description of the experimental spectrum, i.e., the characterization of the real molecular motion consisting of many degrees of freedom activated at finite temperature, often strongly coupled and anharmonic in nature (see Refs. [13–15] for comparative

studies with the static methods). Concerning the static methods that constitute the point of this work, their performances, as a compromise between reliability and computational time, are still not as well established as electronic structure theory. This particularly results from the fact that the quality of the results and the computational feasibility of the system under investigation depend on at least two limiting steps: the nature of the potential energy surface (PES) and the way to solve the subsequent vibrational Schrödinger equation. Whatever the method of electronic structure calculation used, the large dimension of the PES (M dimensions corresponding to the number of vibrational modes) requires a representation that makes feasible the treatment of large molecules. In this connection, the first approach consists of expanding the potential energy in a Taylor series in normal coordinates (q_i) around the equilibrium geometry generally truncated at fourth order:

$$V(q_1, \ldots, q_M) = \frac{1}{2} \sum_{i=1}^{M} \omega_i q_i^2 + \sum_{i=1}^{M} \sum_{j \leq i}^{M} \sum_{k \leq j}^{M} k_{ijk} q_i q_j q_k$$
$$+ \sum_{i=1}^{M} \sum_{j \leq i}^{M} \sum_{k \leq j}^{M} \sum_{l \leq k}^{M} k_{ijkl} q_i q_j q_k q_l + \cdots \quad (1)$$

Drawbacks to this approach are the unphysical behavior of the expansion in the limit of large values of the normal coordinates and the uncertainty in the radius of convergence of such an expansion. About 10 years ago, an alternative suggestion based on a hierarchical representation of the N-mode potential energy was introduced [16]:

$$V(q_1, \ldots, q_M) = \sum_{i=1}^{M} V^1(q_i) + \sum_{i=1}^{M} \sum_{j \leq i}^{M} V^2(q_i, q_j)$$
$$+ \sum_{i=1}^{M} \sum_{j \leq i}^{M} \sum_{k \leq j}^{M} V^3(q_i, q_j, q_k)$$
$$+ \sum_{i=1}^{M} \sum_{j \leq i}^{M} \sum_{k \leq j}^{M} \sum_{l \leq k}^{M} V^4(q_i, q_j, q_k, q_l) \quad (2)$$

This more flexible potential allows a better description of the modes far from the equilibrium geometry and a better representation of the floppy modes, generally lying below, say 600 cm^{-1}. A polynomial expansion of the sequence V^i truncated at fourth order relies on the Taylor series expressed above. More generally, the expansion of the potential can be characterized by the convention nMmT, specifying an m-order Taylor expansion coupling a maximum of n modes [11]. This has the practical advantage of allowing multidimensional integrals over vibrational wave functions to be factorized into products of one-dimensional integrals. Furthermore, the discarding of the n-mode interactions involving more than three-modes, in principle very weak, decreases substantially the required

number of electronic structure computations. This allows the treatment of larger molecular systems [17–21] which are fairly well described in the mid infrared region. The subsequent limiting step is the (ro)vibrational treatment of the anharmonicity. Roughly, four approximate schemes have been proposed. The vibrational self consistent field (VSCF) approach represents the total vibrational wave function by a separable product of single mode wave functions optimized separately using an effective mean-field potential [22–24]. For better accuracy, the correlation between modes is commonly treated by second-order perturbation theory (VPT2) [25, 26] (or vibrational second-order Møller-Plesset (VMP2) [27]) and the vibrational configuration interaction (VCI) [28–30] approaches or, more recently, by the vibrational coupled cluster (VCC) [31] level of theory. According to the author, the VCC approach is size-extensive (unlike VCI), provides a hierarchy where convergence towards the full VCI (FVCI) limit is ensured (unlike VMPn series) which yields promising results from an algorithm whose the optimization is still in progress. The VMP2 approach provides straightforwardly closed expressions for most of the spectroscopic parameters required for the analysis of the experimental frequencies and appears very effective for the study of polyatomic molecules of medium dimension since it is not hampered by a diagonalization procedure. Nevertheless, the VMP2 approach overestimates the strong anharmonic couplings (Fermi or Darling-Dennisson resonances). Attempts to correct the numerical instabilities were proposed [32–34]; typically they consisted of deleting the resonance interaction from the second-order perturbation equation [35–37]) and to treat it more correctly by a separate diagonalization of its 2 × 2 Hamiltonian matrix representation. The widespread VCI treatment includes explicit interactions between the modes (like VMP2) and consists of the diagonalization of the Hamiltonian matrix representation containing the wave functions under investigation (S_0 subspace) and their multiexcitations (S_1 subspace). The method is exact for a given Hamiltonian but extremely time-consuming due to the very large number of basis functions required for obtaining fully converged values. On that point, the need for quadruple excitations VCI$_{SDTQ}$ and even more for a refined representation of X–H stretching modes leads to a dramatic increase of the CI matrices for larger molecules. To be computationally much cheaper, the challenging keypoint consists in finding a recipe that massively truncates the basis set to generate an active space allowing a minimum loss of correlation energy that consists at reducing the space of investigation or at selecting the most pertinent interacting configurations with the subspace of interest. For the first, the reduction of the S_0 subspace consists of a process, easily parallelisable, that splits the overall space of interest into several spectral windows followed by the construction of smaller CI

matrices [38, 39]. The maximum reduction is reached for the 'state by state' or 'specific-state' treatment that requires $3N - 5$ individual VCI calculations [40] for the investigation of the fundamental transitions. The additional price for these enhanced convergences is the non-orthogonality of the VCI wavefunctions, which impacts on the computation of transition properties. On that point, the fair treatment of IR (or Raman) intensities requires not only the anharmonic description of the $3N - 6$ fundamental modes but also the description of the multiexcitations strongly connected with them. Thus, the best compromise between computational time and accuracy is reached by including in the state-specific treatment, the configurations that also describe the multiexcitations IR or Raman actives. This particular aspect is the keypoint of the algorithm presented in this paper. Concerning the reduction of the S_1 subspace, attempts to discard the multiexcitations based exclusively on energy or degree criteria lead to erroneous results [41, 42]. A more flexible approach, first applied in electronic structure theory [43], resides in the selection of the active space with respect to the coupling strengths between the wave functions under investigation and their multiexcitations [44–47]. One selection scheme starts from the screening of the potential function: a given n-mode term can lead, through the application of creation and annihilation operators, to the generation of a set of quasi-degenerate configurations [48, 49]. Another selection scheme is focused on the configuration screening. One of the possibilities is to separate the entire subspace in to tiers (considering a quartic force field, a tier is a set of configurations containing the SDTQ type excitations of a given parent configuration) in which the strongest interactions are evaluated by the second-order perturbational approach [41, 46]. A very recent method, variationally based [40], consists of the separation of the S_1 subspace in to several blocks. The diagonalisation of the first block yields an approximate description of a specific state which is enriched by the successive diagonalisations of the following blocks. The process is ended by a global diagonalization in which the configurations that describe poorly the eigenvector are removed. In a sense, these two concepts are considered in the variation–perturbation process [46]. For a given tier, the strongest interactions evaluated at the VPT2/VMP2 level are allowed to join a CI matrix which is diagonalized and iteratively enriched in the same manner by the screening of the following tiers until the convergence of the desired eigenvalues. The contribution of the weakest interactions is then considered pertubationally. The former and latter types of interaction are referred to as static and dynamic correlation, respectively [50, 51]. Note that the 'Vibrational quasi-degenerate perturbation theory' (VQDPT) method developed by Yagi and coworkers [52] appears, by essence, fairly close to our approach except that no succesive diagonalization scheme

appears in the algorithm; the static correlation is calculated by diagonalizing a VSCF-based CI matrix, which is built by the strongest interactions between a given parent configuration and its quasi-degenerate offspring configurations up to the nth generation from a VMP2 evaluation.

In this work, we present an advanced version of the variation–perturbation algorithm [46] based on an improved selection criterion of the configurations. This code, already tested on a 14 atomic system [21], allows the computation of reliable vibrational properties and requires a minimum amount of effort and machinery (computing power). A more systematic study is performed in the present paper through/ with the following examples: H_2CO, CH_4, $trans$-$C_2H_2F_2$, and C_2H_4O [ethylene oxide(oxirane)] in which the convergence of the fundamental transitions are reported with respect to several configuration selection parameters (maximum excitation level, maximum excitation for each mode, number of modes involved). As an illustration, IR anharmonic intensities are also computed for H_2CO and C_2H_4O. As a benchmark, the computational cost related to vibrational computations of these four molecular systems and of three peptidic bond models: NH_2COCH_3 (acetamide), $NH_2CO(CH_3)_2$ (N-methylacetamide) and $NH_2CO(CH_3)_3$ (N,N-dimethylacetamide) is reported.

2 The method

The vibrational treatment starts from the Watson Hamiltonian for a non-rotating system [53]:

$$\frac{\hat{H}}{hc} = \frac{1}{2}\sum_{i=1}^{M} \omega_i p_i^2 + V(q_1, \ldots, q_M)$$
$$+ \sum_{\alpha} B_\alpha \left(\sum_{i,j \le i, k, l \le k} \zeta_{ij}^\alpha \zeta_{kl}^\alpha q_i p_j q_k p_l \sqrt{\frac{\omega_j \omega_l}{\omega_i \omega_k}} \right) \quad (3)$$

where q_i and p_i are, respectively, the dimensionless normal coordinates and their conjugate momenta. $V(q_1, \ldots, q_M)$ is a polynomial expansion of the PES in terms of normal coordinates q_i truncated at fourth order. The last term represents the major component of the rotational contribution to the anharmonicity: the second-order Coriolis term in which B_α is the rotational constant of the system with respect to the Cartesian axis α and ζ_{ij}^α is the Coriolis constant coupling q_i and q_j through the rotation about the α axis. Thus, the matrix terms of the Hamiltonian representation in the basis set described above are determined analytically [54].

2.1 General algorithm of the VCI-P method

The procedure (see the flow chart shown in Figs. 1, 2) is a state-specific investigation of the vibrational fundamental transitions and combination bands or overtones strongly

connected with them by anharmonic resonances. It requires the iterative construction of $3N - 5$ CI matrices in which at least one vibrational state $\Psi_{i,L}$ per matrix is extracted from each, or more in the case of anharmonic resonances ($i = 0$ for the fundamental level and $i \in [1, M]$ for its mono excitations; L being the number of iterations). The states $\Psi_{i,L}$ are built iteratively by progressive enrichment of the CI matrix with the most pertinent interactions. Thus, by successive diagonalizations, the procedure yields an approximate wave-function $\Psi_{i,l}$ related to the lth iteration until the convergence of its corresponding energy $\varepsilon_{i,l}^{VCI-P}$. For any iteration l, the vectors are linear combinations of vibrational configurations:

$$\Psi_{i,l} = \sum_j c'_{ij} \Phi_j^{n_j} \tag{4}$$

with

$$\Phi_j^{n_j} = \prod_{k=1}^{M} \phi_k^{n_{kj}} \tag{5}$$

a product of harmonic oscillators (HO) for which the excitation with respect to a configuration $\Phi_j^{n_j}$ is

$$N_i^j = |n_j - n_i| = \sum_{k=1}^{M} |n_{jk} - n_{ik}| \tag{6}$$

$n_{\alpha\beta}$ being the quantum number related to the oscillator β in the configuration α. Thus, the CI matrix is composed of two subspaces: the S_0 subspace, typically of one-dimension in absence of resonances, containing the configuration of interest $|\Phi_i^{n_i}\rangle^{S_0}$ and the S_1 subspace, containing the selected

Fig. 1 flow chart of the VCI-P algorithm: part 1

$$\%WF_n = \frac{\%WF_{n-1}}{\alpha \in [1;2]}$$

$$\%WF_n \rightarrow N_{|\Phi_{strong}\rangle}$$

if $N_{|\Phi_{strong}\rangle} \geq S_{1max}$ then $N_{|\Phi_{strong}\rangle} = S_{1max}$:

$$\%WF_n = \sum_k^{S_{1max}} c_{ik_n}^2$$

if $N_{|\Phi_{strong}\rangle} \leq \frac{S_{1max}}{3}$ then $N_{|\Phi_{strong}\rangle} = \frac{S_{1max}}{3}$:

$$\%WF_n = \sum_k^{\frac{S_{1max}}{3}} c_{ik_n}^2$$

CI size=CI size+$N_{|\Phi_{strong}\rangle}$

diagonalisation :

$$\varepsilon_{i,n}^{VCI}$$

$$\varepsilon_{i,n}^{VCI-P} = \varepsilon_{i,n}^{VCI} + \sum_{weak} \frac{\langle \Psi_{i,n}|\hat{H}|\Phi_{weak}\rangle^2}{\varepsilon_{i,n}^{VCI} - E_{weak}^0}$$

no — $conv_n \leq conv$

yes

no — $i = 3N_{atom} - 5$

yes

END
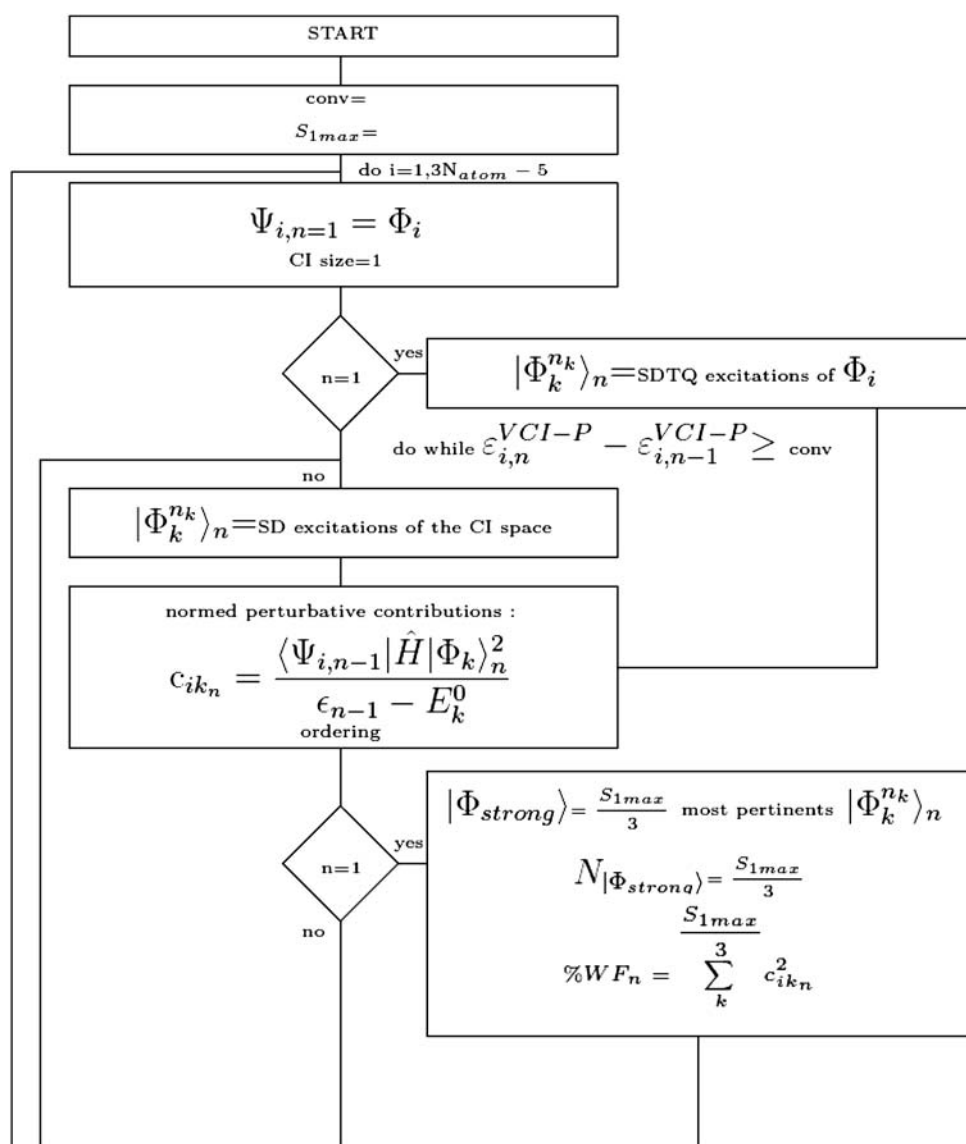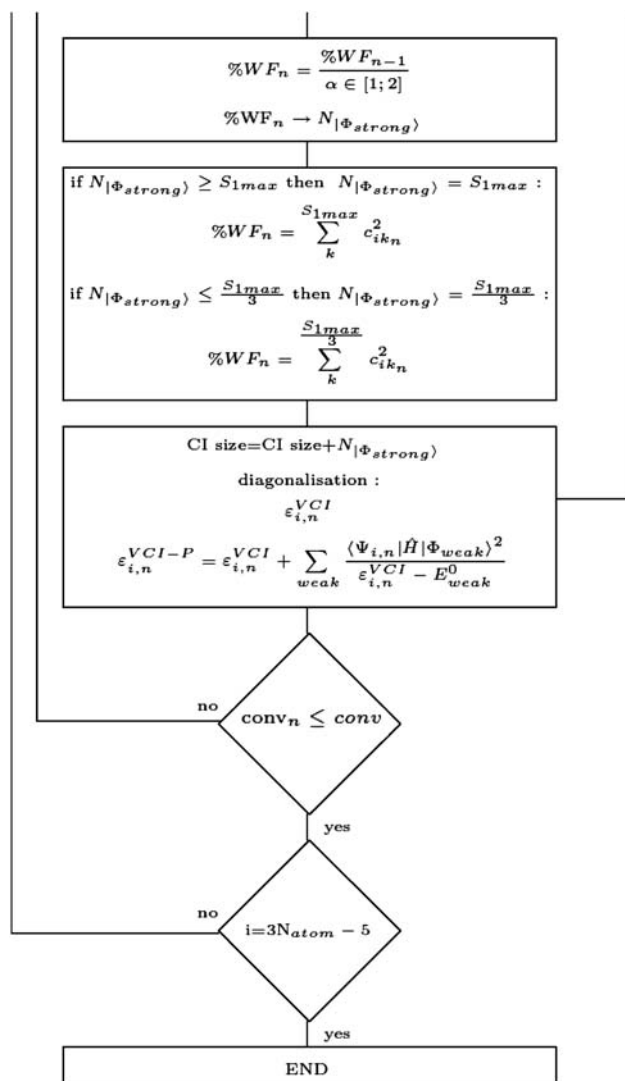
Fig. 2 flow chart of the VCI-P algorithm: part 2

configurations during the previous iterations $\left(|\Phi_j^{n_j}\rangle_{l-1}^{S_1}\right)$. Additional multiexcitations $\left(|\Phi_{strong}^{n_{strong}}\rangle_l\right)$ of these configurations, no higher than the fourth, are then selected by calculating their impact on the approximate wave function $\Psi_{i,l-1}$ using the MP2 level of theory [35]:

$$c_{ik_l} = \frac{\langle \Psi_{i,l-1}|\hat{H}|\Phi_k^{n_k}\rangle_l^2}{\epsilon_{l-1} - E_k^0} \tag{7}$$

with ε_{l-1} and E_k^0, the eigenvalues associated to the eigenvectors $|\Psi_{i,l-1}\rangle$ and $|\Phi_k^{n_k}\rangle_l$, respectively. Note that $|\Phi_k^{n_k}\rangle_l$ is considered as 'strong' or 'weak' according to the value c_{ik_l}.

From the lth diagonalization, the configurations $|\Phi_j^{n_j}\rangle_l$ having c_{ij}^2 (see Eq. 4) greater than a threshold defined by the user are considered as strong resonant configurations. They are inserted in the S_0 subspace in which the convergence of their VCI-P energy is proceeded. This ensures for each CI matrix, the orthogonality between the state $\Psi_{i,L}$ and their

connected states through Fermi resonances for which the correspondings anharmonic intensities can be determined more safely. However, the non-orthogonality between pairs of states is necessary limited since the overlap between their respective CI spaces is important, the major configurations involved in the description of each state being all present in both CI spaces.

A second threshold, discussed in the next subsection, manages the insertion of the configurations $|\Phi_{strong}^{n_{strong}}\rangle_l$ into the S_1 subspace and the discarding of the weakest contributions $|\Phi_{weak}^{n_{weak}}\rangle_l$ arising from the generated configurations $|\Phi_k^{n_k}\rangle_l$. Then, the overall contribution of the weakest interactions to $\Psi_{i,l}$ is calculated perturbationally. This gives rise to the VCI-P energy:

$$\varepsilon_{i,l}^{VCI-P} = \varepsilon_{i,l}^{VCI} + \sum_{weak} \frac{\langle \Psi_{i,l}|\hat{H}|\Phi_{weak}^{n_{weak}}\rangle_l}{\varepsilon_{i,l}^{VCI} - E_{weak}^0}. \tag{8}$$

2.2 Generation and selection of the multiexcitations

The generation is governed by a first set of three thresholds: (i) $N_0^{j_{max}}$ is the maximum multiexcitation number with respect to the fundamental level for the overall procedure, (ii) $N_j^{k_{max}}$ is the maximum multiexcitation number that allows to generate the $|\Phi_k^{n_k}\rangle_l$ configurations from the $|\Phi_j^{n_j}\rangle_l$ for the lth iteration, and (iii) the number of modes involved in the multiexcitation. Considering the expansion of the PES, the two last thresholds are set to 4 and 3, respectively. As notation, a VCI$_{SDTQ}$ computation of the fundamental transitions is noted VCI$\left[3, N_0^{j_{max}} = 5\right]_0$ (from the ground state) or VCI$\left[3, N_0^{j_{max}} = 4\right]_s$ (from the state of interest). For the VCI-P method, $N_j^{k_{max}}$ is added in the notation to inform about the nature of the subspace generated for each iteration l. Here, the starting point is the VCI-P $[(3, 4)_l, 13]_0$ computation which is an iterative generation of the SDTQ excitations with at most 3-mode couplings up to the 13-excitations from the ground state.

The space of the configurations $|\Phi_k^{n_k}\rangle_l$ can be too large to be entirely stored in matrix or read efficiently on file. The basic idea is to evaluate 'on the fly' with Eq. 7 their perturbative contribution and to store only the contributions greater than a first threshold, initially set to the very low value of 10^{-7}. Thus, the relative contribution of each $|\Phi_k^{n_k}\rangle_l$ to the state $|\Psi_{i,l-1}\rangle$ for the iteration l can be determined. This allows the determination of a very restricted active space comprised of all the leading configurations: the incoming subspace $|\Phi_{strong}^{n_{strong}}\rangle_l$ for each iteration must be both sufficiently large to ensure a rapid convergence and sufficiently small to allow the insertion of higher excitations for the further iterations. As matter of fact, the size of this incoming subspace is always between two thrust values (S_{1max} and $S_{1min} = S_{1max}/3$). For the first iteration, the first

S_{1min} configurations are selected, and the sum of their relative contribution (%WF) is kept as a parameter for the next iteration. Then, for any iteration, the parameter %WF provides the size of the incoming subspace if the value is comprised between S_{1max} and S_{1min}. For any other case, this parameter is set to the %WF corresponding to S_{1max} or S_{1min}, depending on whether the number of the incoming configurations appear above or below these values, respectively (see Figs. 1, 2).

3 Computational details

Structural optimization, harmonic frequencies, harmonic IR intensities, and quartic force field calculations were performed with the Gaussian 03 program [55]. Electronic structure calculations were performed at the CCSD(T) [56]/cc-pVTZ [57] level of theory for H_2CO, CH_4, trans-$C_2H_2F_2$, and C_2H_4O and at the DFT level using the B3LYP [58–60] functional with a valence double zeta Pople basis set which includes diffuse and polarization functions, 6–31 + $G(d, p)$ for the larger molecular systems. This model chemistry was chosen since it has been previously shown [61, 62] that for the prediction of harmonic and anharmonic force constants for small organic systems, it is able to reproduce the results obtained using the more expensive CCSD(T)/cc-pVTZ level of theory, with an average error (difference) of 10 cm^{-1} on the fundamental transitions.

The analytical model of the potential functions is determined as follows [33]: for a minimum energy structure for a given system, a quartic force field is built in which the third and fourth derivatives are computed by $6N - 11$ (N = number of atoms) numerical differentiations of analytical second derivatives. This method is suitable only for all computational models for which analytical second derivatives are available. In the quartic approximation, the potential provided by the Gaussian code is a Taylor series in normal coordinates limited to the 3-mode interactions. From a technical point of view, it can be shown [33] that the best setup is obtained using a step size of 0.01 Å for the numerical differentiation of harmonic frequencies, tight convergence criteria for structural optimizations and fine grids for integral evaluation (i.e., at least 99 radial and 590 angular points).

The anharmonic vibrational treatment is performed with the locally developed Fortran 90 code [63] described above for the computations of the VCI-P energies. Furthermore, this program allows the computation of anharmonic intensities, as reported in the references [64, 65]: starting from the quadratic expansion of the dipole surface, the second derivatives of dipole moment, $d_{\alpha ij}$ (where α is a Cartesian component of the dipole moment vector $d_{\alpha j}$

referred to the Eckart axes) are calculated in a manner analogous to the cubic and quartic force constants detailed above:

$$D_\alpha = D_\alpha(0) + \sum_i d_{\alpha i} q_i + \frac{1}{2} \sum_{i,j} d_{\alpha ij} q_i q_j \qquad (9)$$

The anharmonic intensity between an initial state i and a final state j is then evaluated as follows:

$$I_{i,j} = \frac{8\pi^3 N_A}{3hc(4\pi\varepsilon_0)} v_{0,i} \sum_\alpha \langle \Psi_{i,N} | D_\alpha | \Psi_{j,N} \rangle^2 (N_i - N_j) \qquad (10)$$

Here, caution is taken by including the entire description of the fundamental state $\Psi_{i,N}$ into the $3N - 6$ CI spaces which describe the states $\Psi_{j,N}$.

4 Results and discussion

4.1 Convergence with respect to the size of the CI matrix

VCI-P computations for H_2CO and CH_4 were performed for several values of S_{1max} and compared with their full VCI (FVCI) counterpart. The so-called FVCI computations are performed by diagonalization of CI matrices comprising configurations ranging from the fundamental to its 13-multiexcitations with no restriction on the number of modes simultaneously excited (VCI $[6, 13]_0$ and VCI $[9, 13]_0$, respectively). This yields CI matrices containing 27,132 and 293,930 configurations for H_2CO and CH_4, respectively, in which the 25 first eigenvalues are provided by a Davidson procedure [66]. The results are reported in Table 1 in terms of signed discrepancies with respect to ∼FVCI computations for the fundamental transitions of the two systems and the combination band ($v_3 + v_6$) for H_2CO because of its strong anharmonic coupling with the v_5. Information in brackets provides the number of iterations required for convergence of the eigenvalues for each specific state investigated for which the convergence criterion has been set to the very tight value of 0.1 cm^{-1}. Furthermore, the size of the matrices resulting from such a process is reported in parentheses. Globally, the iterative process yields quite well-converged values for the two systems, whatever the size of the matrices. This emphasizes the stability of the selection scheme proposed. Even though the generation of very small CI matrices does not save further computational time for $S_{1max} = 10$, due to the number of iterations required for obtaining the converged VCI-P energies, the process is a good compromise between accuracy and computational time for low values of S_{1max}. $S_{1max} = 150$ was set up for all the next illustrations.

Table 1 VCI-P $[(3, 4)_n, 13]_0$ results (in cm^{-1}) with respect to $\sim$FVCI results (see text) and with respect to several maximum sizes of the incoming subspace for each iteration: examples of H$_2$CO and CH$_4$

	S_{1max}	10	50	100	150	200	250	VCI $[M, 13]_0 \sim$ FVCI
H$_2$CO	v_4	0.08	0.07	0.07	0.07	0.07	0.07	1,168.47
		[7]	[5]	[5]	[5]	[5]	[5]	
		(41)	(96)	(22)	(345)	(465)	(601)	
	v_6	0.08	0.02	0.02	0.02	0.02	0.02	1,249.13
		[10]	[6]	[6]	[5]	[5]	[5]	
		(47)	(153)	(314)	(372)	(491)	(616)	
	v_3	0.23	0.08	0.08	0.08	0.08	0.08	1,506.73
		[11]	[7]	[6]	[6]	[5]	[5]	
		(42)	(191)	(317)	(510)	(487)	(616)	
	v_2	0.09	0.06	0.06	0.06	0.06	0.06	1,749.43
		[11]	[7]	[6]	[6]	[5]	[5]	
		(72)	(205)	(349)	(522)	(491)	(624)	
	v_1	0.12	0.05	0.02	0.02	0.02	0.02	2,789.68
		[17]	[8]	[6]	[6]	[6]	[6]	
		(125)	(249)	(360)	(556)	(778)	(975)	
	v_5	0.26	0.17	0.15	0.15	0.15	0.15	2,854.34
		[17]	[8]	[7]	[6]	[6]	[6]	
		(152)	(306)	(511)	(616)	(821)	(1,026)	
	$v_3 + v_6$	0.42	0.29	0.25	0.23	0.23	0.23	2,710.57
CH$_4$	v_4	0.15	0.29	0.25	0.22	0.21	0.21	1,307.35
		[15]	[7]	[6]	[6]	[6]	[5]	
		(132)	(256)	(411)	(616)	(821)	(776)	
	v_2	0.61	0.40	0.39	0.38	0.38	0.38	1,530.08
		[7]	[6]	[6]	[6]	[6]	[5]	
		(52)	(256)	(386)	(563)	(743)	(671)	
	v_1	1.90	0.70	0.49	0.49	0.49	0.49	2,923.76
		[13]	[11]	[16]	[11]	[9]	[9]	
		(93)	(416)	(1,109)	(1,126)	(1,158)	(1,207)	
	v_3	1.41	1.00	0.62	0.45	0.45	0.45	3,032.01
		[17]	[11]	[15]	[13]	[11]	[10]	
		(152)	(438)	(1,222)	(1,553)	(1,645)	(1,820)	

Number of iterations are shown in square brackets; final size of the CI matrix are shown in parentheses

4.2 Convergence with respect to the multiexcitations of the ZPE

From a quartic expansion in Taylor series of the PES, a fair convergence of the anharmonic values is generally not reached from a VCI$_{SDTQ}$ treatment $\left(N_0^{j_{max}} = 5\right)$, namely for states exhibiting Fermi or Darling-Dennisson resonances. The previously reported values were obtained by allowing the generation of configurations up to $\left(N_0^{j_{max}} = 13\right)$, but such excitations could have a weak impact on the vibrational energies. This is illustrated by the Table 2 by some noteworthy results for H$_2$CO, CH$_4$, trans-C$_2$H$_2$F$_2$, and C$_2$H$_4$O (oxirane) for $N_0^{j_{max}} = 5$–13. It reveals that converged values are reached for $N_0^{j_{max}} = 9$, i.e., where the description of the SDTQ excitations of the vibrational

states is improved by their own SDTQ excitations. Indeed we note, through these examples, some values which can vary by more than 40 cm^{-1} as well as some assignment inversions for strongly coupled states, namely the case of the trans-C$_2$H$_2$F$_2$ system for the v_{10} and $(v_3 + v_6)$ states.

4.3 Convergence with respect to the nature of the incoming configurations

The setting of $\left(N_j^{k_{max}}\right)$ allows the generation of a specific type of multiexcitations. Concerning the previous illustrated results in Sect. 4.2, the SDTQ-excitations of the CI space were generated for each iteration. The influence of the three kinds of generation (SDTQ, SDT, and SD type) is illustrated through the investigation of the v_1 transition for

Table 2 VCI-P $\left[(3,4)_n, N_0^{j_{max}}\right]_0$ results (in cm^{-1}) with respect to VCI-P $[(3, 4)_n, 13]_0$

	$N_0^{j_{max}}$	5	7	9	11	13
H$_2$CO	$\tilde{v}_{<2,500}$	0.35	0.05	0.00	0.00	–
	v_1	2.07	1.37	0.00	0.00	2,789.71
	v_5	2.22	0.91	0.00	0.00	2,854.54
	$v_3 + v_6$	3.96	0.31	0.01	0.00	2,710.90
CH$_4$	$\tilde{v}_{<2,500}$	0.34	0.04	0.00	0.00	–
	v_1	2.17	0.21	0.00	0.00	2,923.76
	v_3	1.49	0.14	0.00	0.00	3,032.01
t-C$_2$H$_2$F$_2$	$\tilde{v}_{<1,700}$	0.76	0.33	0.03	0.03	–
	v_{10}	−3.63	2.34	0.26	0.26	1,706.32
	$v_3 + v_6$	12.05	−0.41	0.14	0.14	1,698.38
	$2v_5$	–	7.60	1.45	0.40	1,693.42
	v_{11}	−0.42	0.58	0.03	0.00	3,121.13
	$v_8 + v_{10}$	7.79	0.64	0.02	0.02	2,959.45
	$v_3 + v_8 + v_9$	–	0.61	0.03	0.00	3,129.64
	v_{12}	2.16	−9.76	0.74	0.00	3,107.55
	$v_9 + v_{10}$	11.33	0.77	−0.15	−0.15	2,986.70
C$_2$H$_4$O	$\tilde{v}_{<2,500}$	0.29	0.10	0.00	0.00	–
	v_9	4.70	0.67	0.01	0.00	2,921.23
	$v_2 + v_{10}$	5.70	0.68	0.02	0.00	3,031.62
	v_1	8.04	2.35	0.57	0.56	2,929.09
	$2v_{10}$	7.13	0.77	0.16	0.00	2,963.26
	$2v_2$	12.90	0.28	0.11	0.10	3,011.18
	v_6	9.20	0.75	0.02	0.00	3,031.98
	$v_8 + v_{11} + v_{12}$	–	0.46	0.02	0.00	3,055.29
	v_{13}	−2.64	0.45	0.03	0.00	3,042.71
	$v_4 + v_8 + v_{12}$	42.36	0.55	0.04	0.00	3,031.67
	$v_7 + v_8 + v_{15}$	–	0.44	0.07	0.00	3,052.55

$N_0^{j_{max}}$ being the maximum multiexcitation number allowed

oxirane. The v_1 fundamental transition is involved in two strong Fermi resonances, with the $2v_{10}$ and $2v_2$ states. This can be seen in the resulting composition of the three states after the anharmonic analysis has been performed. Here the process starts with the most pertinent SDTQ excitations of the states of interest for the first iteration followed by a SDTQ, SDT or SD type generation for the next iterations. Whatever the generation type, the three corresponding eigenvalues and the estimation of the v_1 character are identical:

SDTQ type generation: $E(\Psi_{1,L}) = 15{,}393.35$ cm^{-1}
$c_{v_1,\omega_1} = 0.576, c_{2v_{10},\omega_1} = -0.570, c_{2v_2,\omega_1} = 0.376$
SDT type generation: $E(\Psi_{1,L}) = 15{,}393.24$ cm^{-1}
$c_{v_1,\omega_1} = 0.579, c_{2v_{10},\omega_1} = -0.563, c_{2v_2,\omega_1} = 0.374$
SD type generation: $E(\Psi_{1,L}) = 15{,}393.35$ cm^{-1}
$c_{v_1,\omega_1} = 0.580; c_{2v_{10},\omega_1} = -0.569; c_{2v_2,\omega_1} = 0.375$

The main differences reside in the computational cost with respect to the number of iteration, as depicted in Fig. 3. For a given iteration n, the generated set of configurations must be sufficiently small to limit the computational cost of their MP2 evaluation, but sufficiently pertinent to avoid a brutal increase of the matrix size during the next iteration. This discards the generation of the Q excitations for which the main part of the process is devoted to their MP2 evaluation. The SD type generation (VCI-P $[(2, 2)_n, 13]_0$), also tested for the entire set of illustrated frequencies, appears as a good compromise to further save computational time.

4.4 Anharmonic intensities

The computation of anharmonic intensities provided by the VCI-P program is illustrated through the examples of H$_2$CO and C$_2$H$_4$O. It consists of $3N - 5$ tightened VCI-P computations in which all the configurations $|\Phi_j^{n_j}\rangle_n$ contributing by more than $c_{i,j}^2 = 5\%$ to the first-excited states $\Psi_{i,N}$ are converged energetically in the iterative process. This gives rise to the computation of anharmonic intensities for the first overtones and combination bands having non-zero intensity through their interaction with IR active fundamental transitions. In Table 3, the VCI-P-based results for H$_2$CO are compared with the results of Seidler et al. [67] and Burcl et al. [65] (columns 1–3). All three are DFT-based expansions of the PES and dipole surface with

Fig. 3 Matrix size and relative time (relative time of the first iteration = 1) of the process with respect to the nature of the multiexcitations generated: example of the v_1 for C_2H_4O
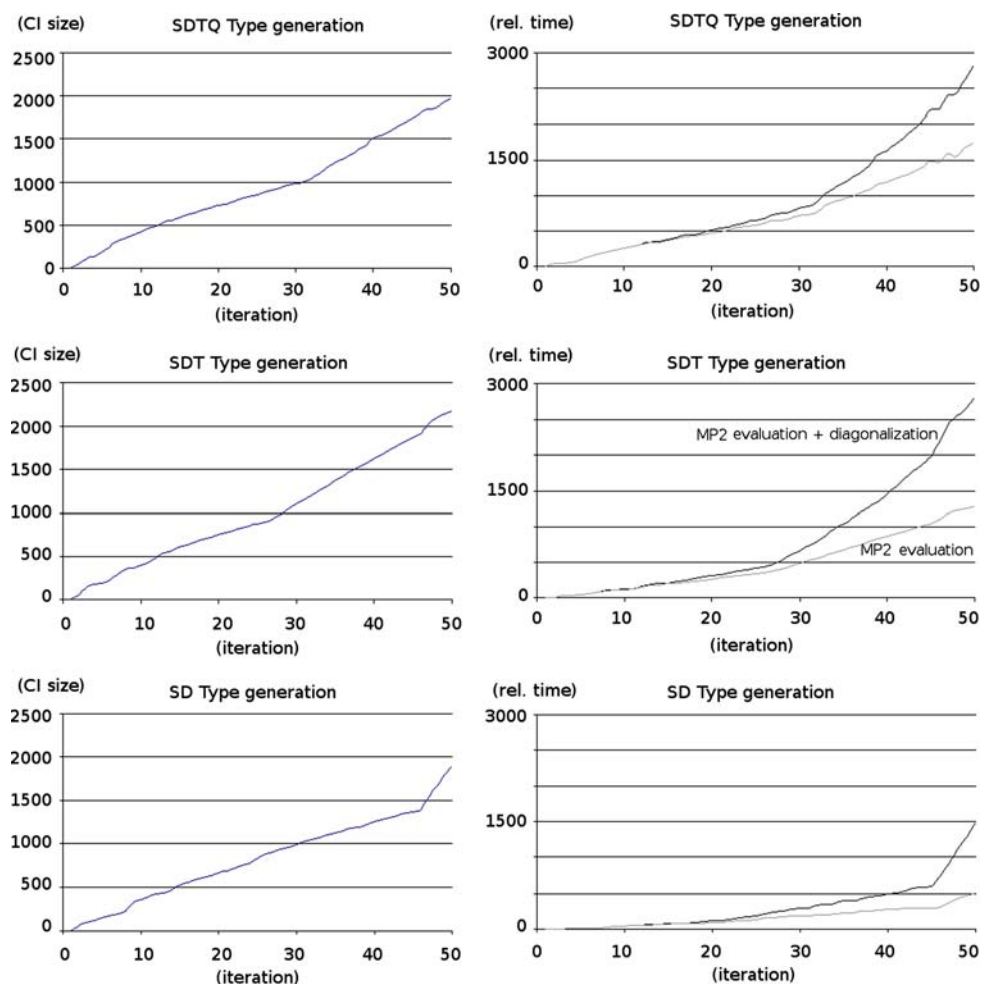
Table 3 Anharmonic intensities (in km mol^{-1}) and anharmonic positions (in cm^{-1}) from several levels of theory for H_2CO: comparison to experimental values

QM method	B3LYP/cc-PVTZ	B3LYP/cc-pVTZ	B97-1/TZ2P	exp[b]		CCSD(T)/cc-pVTZ[c]			
PES expansion	4M4T	3M4T	4M4T			3M4T			
VIB treatment	VSCF + VCI [4, 4]$_s$	HO + VCI [4, 4]$_s$	HO + VCI [4, 4]$_s$			HO + VCI − P [(2, 2)$_n$, 9]$_0$		HO + VCI [6, 13]$_0$	
DS expansion	1M1T	2M2T	3M3T			2M2T[d]		2M2T[d]	
	$A(v)$[a]	$A(v)$[a]	$A(v)$[a]	v	$A(v)$	Δv	$A(v)$	Δv	$A(v)$
v_4	5.55	5.45	4.76	1,167	5.2–6.5	2	4.46	2	4.39
v_6	12.4	10.7	9.66	1,249	9.4–9.9	0	9.28	0	9.28
v_3	10.4	11.1	8.60	1,500	11.2	6	5.01	7	5.00
v_2	120	99.8	107	1,746	74	3	101	3	101
$2v_4$	0.18	0.52	0.002	2,327	0.14	5	0.19	5	0.19
$2v_6$	0.58	1.140	0.83	2,493	0.27	4	0.37	4	0.37
$v_3 + v_6$	36.4	34.2	62.8	2,719	8–14	−8	29.3	−8	29.2
v_1	75.6	72.9	61.7	2,782	48–75.5	7	67.2	7	67.2
v_5	97.0	58.9	59.2	2,843	59–88	11	68.1	11	66.4
$v_2 + v_6$	3.48	4.73	4.97	3,000	0.5–10	9	9.95	9	11.5
$2v_2$	4.31	5.45	3.88	3,472	3.8	10	4.88	10	4.88

[a] See Ref. [67] and therein

[b] See Ref. [69]

[c] Our work

[d] B3LYP/cc-pVTZ model chemistry

Table 4 VCI-P $[(2, 2)_n, 9]_0$ computations for C_2H_4O (ethylene oxyde): harmonic $[A(\omega)]$ and anharmonic $[A_1(v), A_2(v)$: see text] intensities (in km mol^{-1}) with their corresponding anharmonic positions (in cm^{-1})

	$A(\omega)$	$A_1(v)$	$A_2(v)$	VCI-P	Description	P-VMWCI[a]	VMFCI[a]
v_1	14.7	5.3	5.9	2,921	$33.6\%\lvert\omega_1\rangle + 38.2\%\lvert 2\omega_{10}\rangle$	2,922	2,919
$2v_{10}$	0.0	4.6	4.7	2,963	$32.4\%\lvert\omega_1\rangle + 49.6\%\lvert 2\omega_{10}\rangle$		
$2v_2$	0.0	3.1	2.3	3,011	$13.8\%\lvert\omega_1\rangle + 62.4\%\lvert 2\omega_2\rangle$		
v_2	4.5	3.8	3.7	1,502		1,499	1,497
v_3	14.2	11.2	11.2	1,275	$88.4\%\lvert\omega_3\rangle + 4.4\%\lvert 2\omega_3\rangle$	1,271	1,272
$2v_3$	0.0	0.4	0.3	2,545	$4.8\%\lvert\omega_3\rangle + 78.8\%\lvert 2\omega_3\rangle$		
v_4	0.0	0.0	0.0	1,127		1,120	1,123
v_5	77.9	68.9	68.2	884		881	879
v_6	0.0	0.0	0.0	3,032	$56.7\%\lvert\omega_6\rangle + 21.2\%\lvert\omega_8 + \omega_{11} + \omega_{12}\rangle$	3,027	3,032
$v_8 + v_{11} + v_{12}$	0.0	0.0	0.0	3,056	$19.3\%\lvert\omega_6\rangle + 65.8\%\lvert\omega_8 + \omega_{11} + \omega_{12}\rangle$		
v_7	0.0	0.0	0.0	1,154		1,152	1,149
v_8	0.0	0.0	0.0	1,024		1,024	1,019
v_9	37.0	21.8	21.8	2,929	$62.4\%\lvert\omega_9\rangle + 21.4\%\lvert\omega_{10} + \omega_2\rangle$	2,908	2,913
$v_2 + v_{10}$	0.0	5.8	5.8	3,032	$16.0\%\lvert\omega_9\rangle + 51.0\%\lvert\omega_{10} + \omega_2\rangle$		
v_{10}	0.1	0.1	0.1	1,473		1,474	1,468
v_{11}	1.1	1.0	1.0	1,131		1,130	1,125
v_{12}	11.1	10.1	9.6	827		820	823
$v_4 + v_8 + v_{12}$	0.0	5.9	6.6	3,032	$13.0\%\lvert\omega_{13}\rangle + 60.8\%\lvert\omega_4 + \omega_8 + \omega_{12}\rangle$		
v_{13}	47.7	24.7	22.5	3,043	$54.8\%\lvert\omega_{13}\rangle + 16.8\%\lvert\omega_4 + \omega_8 + \omega_{12}\rangle$	3,041	3,041
$v_7 + v_8 + v_{15}$	0.0	4.5	4.3	3,053	$09.6\%\lvert\omega_{13}\rangle + 77.4\%\lvert\omega_7 + \omega_8 + \omega_{15}\rangle$		
v_{14}	3.6	3.6	3.2	1,152		1,151	1,147
v_{15}	0.2	0.2	0.1	800		800	794

Comparison with P-VMWCI and VMFCI treatment from the same hybrid PES [CCSD(T)/cc-pVTZ and B3LYP/6–31 + G(d, p) for the harmonic and the anharmonic part of the quartic force field, respectively]

[a] See Ref. [68]

a VCI method using up to four simultaneously excited modes and up to the four excitations of the states of interest (VCI [4, 4]$_s$). Roughly, these results converge considering the accuracy of the experimental data (column 4). Moreover, it is noteworthy that the VCI-P $[(2, 2)_n, 9]_0$ results (columns 5–6) achieve a perfect convergence with respect to its ~FVCI counterpart both for the frequencies and the IR/VA intensities with a modest basis set (less than 250 HO products vs. 27,132). A further validation test reported in Table 4 was performed for oxirane because of the presence of strong Fermi resonance in the CH stretching region. The set of anharmonic intensities obtained by the purposed method $[A_1(v)]$ in (column 2) is compared to a second set for which the $3N - 5$ CI spaces were concatenated into a single CI space comprising about 10,000 configurations and diagonalized by the Davidson method [66]. The resulting set, called $A_2(v)$ (column 3) do not differ from $A_1(v)$ by more than 1 km mol^{-1} for the largest intensities. As by product, the calculated fundamental transitions are compared to two published post anharmonic treatments [68] with the same PES and reveal the accuracy of the VCI-P method.

4.5 Parallelization of the code and computational cost

The VCI-P program based on $3N - 5$ independent calculations can be easily parallelizable. A parallelization scheme adopted by Rauhut [40] in his state-specific procedure consists of spreading the generation of each VCI matrix over all processors. Here, this choice is hampered by the iterative character of the VCI-P method in which very small CI matrices are generated for the first iterations (see Fig. 3). This leads to a very poor load-balanced algorithm. One prefers the simple static distribution of the $3N - 5$ computations among m processors. Moreover, note that the time saving is not linearly dependent on the number of processors. Concerning this point, strongly anharmonic fundamental modes imply the proper evaluation of their connected (coupled) overtones and combination modes leading to CI matrix sizes that can reach some thousands of configurations. It follows that the time for the treatment could, at most, be reduced to the treatment of the largest CI matrix. On these grounds our distribution consists of one processor for all weakly anharmonic modes plus one processor for each strongly anharmonic mode.

Fig. 4 computational time (in seconds) of the VCI-P $[(2, 2)_n, 9]_0$ process in its parallelized version with respect to the size of the illustrated systems for two sets of thresholds (see text, c_{ij}^2 in %, conv in cm^{-1})
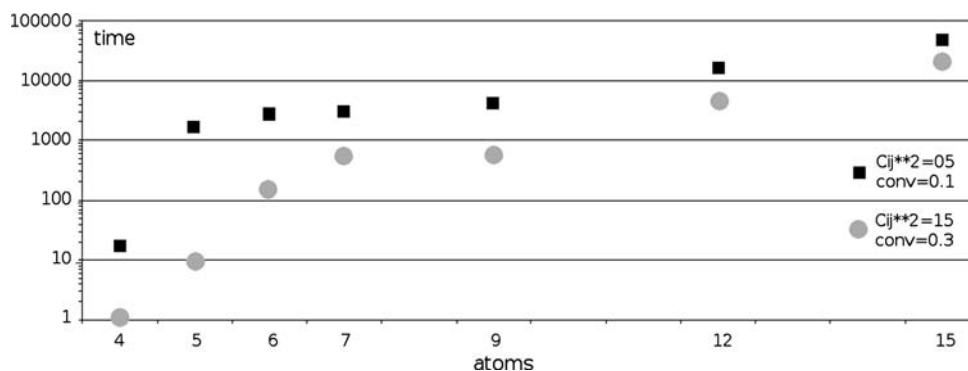
This fixes roughly the number of the required processor to $N + 1$ (N being the number of the X–H stretching modes) for a quite optimized distribution. Thus, 3, 5, 3, 5, 6, 9 and 12 processors (AMD Opteron 2.4 GHz) were used, respectively, for H_2CO, CH_4, *trans*-$C_2H_2F_2$, C_2H_4O, N-H_2COCH_3, $NH_2CO(CH_3)_2$, and $NH_2CO(CH_3)_3$. The total CPU time for the computation of the fundamental transitions, combinations and overtones involved in anharmonic resonances is reported in Fig. 4. Here, two sets of thresholds were considered: the tighter one allows a full description of the IR active overtone and combination transitions that possess a fundamental character greater than 5% with a convergence of 0.1 cm^{-1} on their energy. These criteria were coarsened by a factor of 3 in the second set. This last set of thresolds which allows one to save substantial CPU time is essentially used for a proper evaluation of the fundamental modes and their strongest Fermi resonances. With this procedure, the computational time ranges from 1 s to 6.5 h for the anharmonic vibrational computation of the four-atom up to the 15-atom system illustrated.

5 Conclusions

A variation–perturbation scheme called VCI-P code has been developed for the accurate theoretical description of vibrational resonances in polyatomic molecules. This state-specific process consists of an iterative construction of small $3N - 5$ CI matrices with the most pertinent configurations that describe the states of interest. The perturbative contribution of the overall weakest interactions added to the VCI eigenvalues gives rise to the VCI-P energies. The key point of this article is a recipe that massively truncates the basis set to generate an active space allowing a minimum loss of correlation energy. Through the examples of H_2CO and 1_4, the VCI-P results match the $\sim$FVCI counterparts with a very modest basis set (less than 250 HO products vs. 27,132 for formaldehyde and less than 450 HO products vs. 293,930 for methane). The convergence of the

VCI-P results were also discussed with respect to differents thresholds governing the generation and the selection of the configurations to further optimize the process. Moreover, the code allows an accurate computation of anharmonic intensities by ensuring the orthogonality between the states strongly connected through Fermi of Darling-Dennisson resonances, as illustrated in the example of H_2CO and C_2H_4O. Concerning the parallelization of the code, we propose to spread the $3N - 5$ CI computations on $N + 1$ processors (N being the number of X–H stretching modes) for a quite optimized distribution. Thus, the overall computational time is reduced to the investigation time of the strongest anharmonic modes. This illustrates the accuracy and effectiveness of the VCI-P code.

References

1. Meier R (2005) Chem Soc Rev 34:743
2. Sevegney M, Kannan R, Siedle A, Naik R, Naik V (2006) Vib Spectrosc 40:246
3. Gagarinov A, Degtyareva O, Khodonov A, Terpugov E (2006) Vib Spectrosc 42:231
4. Schweitzer-Stenner R (2006) Vib Spectrosc 42:98
5. Xie W, Ye Y, Shen A, Zhou L, Lou Z, Wang X, Hu J (2008) Vib Spectrosc 47:119
6. Aliaga A, Osorio-Roman I, Garrido C, Leyton P, Cárcamo J, Clavijo E, Gómez-Jeria J, G F, Campos-Vallette M (2008) Vib Spectrosc
7. Zhao W, Gao X, Hao L, Huang M, Huang T, Wu T, Zhang W, Chen W (2007) Vib Spectrosc 44:388
8. Portnov A, Ganot Y, Bespachiansky E, Rosenwaks S, Bar I (2006) Vib Spectrosc 42:147
9. Crim F (1996) J Phys Chem 100:12725
10. Åstrand P, Ruud K, Taylor P (2000) J Chem Phys 112:2655
11. Kongsted J, Christiansen O (2006) J Chem Phys 125:124108
12. Berens P, Wilson K (1981) J Chem Phys 74:4872
13. Rega N (2006) Theor Chem Acc 116:347

14. Carbonniere P, Dargelos A, Ciofini C, Adamo C, Pouchan C (2009) Phys Chem Chem Phys 21:4375
15. Pouchan C, Carbonniere P (2009) Chin J Chem Phys 22:123
16. Carter S, Bowman J, Handy N (1998) Theor Chem Acc 100:191
17. Burcl R, Handy N, Carter S (2003) Spectro Chem Acta Part A 59:1881
18. Miani A, Cané E, Palmieri P, Trombetti A, Handy N (2000) J Chem Phys 112:248
19. Boese A, Martin J (2004) J Phys Chem A 108:3085
20. Barone V, Festa G, Grandi A, Rega N, Sanna N (2004) Chem Phys Lett 388:279
21. Carbonniere P, Pouchan C (2008) Chem Phys Lett 462:169
22. Carter S, Culik S, Bowman J (1997) J Chem Phys 107:10458
23. Bowman J, Christoffel K, Tobin F (1979) J Phys Chem 83:905
24. Jung J, Gerber R (1996) J Chem Phys 105:10332
25. Clabo D, Allen W, Remington R, Yamaguchi Y, Schaefer III H (1988) Chem Phys 123:187
26. Dressler S, Thiel W (1997) Chem Phys Lett 273:71
27. Christiansen O (2003) J Chem Phys 119:5773
28. Dunn K, Boggs J, Pulay P (1986) J Chem Phys 85:5838
29. Cassam-Chenai P, Lievin J (2006) J Comput Chem 27
30. Ribeiro F, Iung C, Leforestier C (2005) J Chem Phys 123:054106
31. Christiansen O (2004) J Chem Phys 120:2149
32. Martin J, Lee T, Francois J (1995) J Chem Phys 103:2589
33. Barone V (2005) J Chem Phys 122:014108
34. Danecek P, Bour P (2007) J Comput Chem 28:1617
35. Møller C, Plessetv (1934) Phys Rev 46:618
36. Nielsen H Rev Mod Phys 23
37. Willets A, Handy N (1995) Chem Phys Lett 235:286
38. Carbonniere P (2002) PhD Thesis, University of Pau
39. Gohaud N, Begue D, Darrigan C, Pouchan C (2005) J Comput Chem 26:743
40. Rauhut G (2007) J Chem Phys 127:184109
41. Iung C, Leforestier C, Wyatt R (1993) J Chem Phys 98:6722
42. Christiansen O, Luis J (2005) Int J Quantum Chem 104
43. Buenker R, Peyerimhoff S, Buthsher W (1978) Mol Phys 35:771
44. Stuchebrukhov A, Marcus R (1993) J Chem Phys 98:6044
45. Gaw JF, Willets A, Green WH, Handy NC, Bowmann JM (1990) Advanced molecular vibrations and collision dynamics, vol IB. JAI, Greenwich, CT
46. Pouchan C, Zaki K (1997) J Chem Phys 107:342
47. Scribano Y, Benoit D (2008) Chem Phys Lett 458:384
48. Wyatt R (1985) Chem Phys Lett 121:301
49. Chang J, Moiseyev N, Wyatt R (1986) J Chem Phys 84:4997
50. Hirao K (1991) Chem Phys Lett 190:374
51. Nakano H (1993) J Chem Phys 99:7983
52. Yagi K, Hirata S, Hirao K (2008) Phys Chem Chem Phys 10:1781
53. Watson J (1968) Mol Phys 15:479
54. Carbonniere P, Barone V (2004) Chem Phys Lett 392:365
55. Frisch MJ, Trucks GW, Schlegel HB, Scuseria GE, Robb MA, Cheeseman JR, Montgomery JJA, Vreven T, Kudin KN, Burant JC, Millam JM, Iyengar SS, Tomasi J, Barone V, Mennucci B, Cossi M, Scalmani G, Rega N, Petersson GA, Nakatsuji H, Hada M, Ehara M, Toyota K, Fukuda R, Hasegawa J, Ishida M, Nakajima T, Honda Y, Kitao O, Nakai H, Klene M, Li X, Knox JE, Hratchian HP, Cross JB, Bakken V, Adamo C, Jaramillo J, Gomperts R, Stratmann RE, Yazyev O, Austin AJ, Cammi R, Pomelli C, Ochterski JW, Ayala PY, Morokuma K, Voth GA, Salvador P, Dannenberg JJ, Zakrzewski VG, Dapprich S, Daniels AD, Strain MC, Farkas O, Malick DK, Rabuck AD, Raghavachari K, Foresman JB, Ortiz JV, Cui Q, Baboul AG, Clifford S, Cioslowski J, Stefanov BB, Liu G, Liashenko A, Piskorz P, Komaromi I, Martin RL, Fox DJ, Keith T, Al-Laham MA, Peng CY, Nanayakkara A, Challacombe M, Gill PMW, Johnson B, Chen W, Wong MW, Gonzalez C, Pople JA (2004) Gaussian 03, Revision E.01, Gaussian, Inc., Wallingford, CT
56. Raghavachari K, Trucks G, Pople J, Head-Gordon M (1989) Chem Phys Lett 157:479
57. Kendall R, Dunning T Jr, Harrison R (1992) J Chem Phys 96:6796
58. Becke A (1993) J Chem Phys 98:5648
59. Lee C, Yang W, Parr R et al (1988) Phys Rev B 37:785
60. Vosko S, Wilk L, Nusair M (1980) Can J Phys 58:1200
61. Carbonniere P, Barone V (2004) Chem Phys Lett 399:226
62. Carbonniere P, Lucca T, Pouchan C, Rega N, Barone V (2005) J Comput Chem 26:284
63. Carbonniere P, Dargelos A (2008) VCI-P, a time independant treatment of anharmonicity from a variation-perturbation approach, IPREM, UMR 5254, Pau, France
64. Baraille I, Larrieu C, Dargelos A, Chaillet M (2001) Chem Phys 273:91
65. Burcl R, Carter S, Handy NC (2003) Chem Phys Lett 380:237
66. Davidson E (1975) J Comput Phys 17:87
67. Seidler P, Kongsted J, Christiansen O (2007) J Phys Chem A 111:11205
68. Bégué D, Gohaud N, Pouchan C, Cassam-Chenaï P, Liévin J (2007) J Chem Phys 127:164115
69. Reisner D, Field R, Kinsey J, Dai H (1984) J Chem Phys 80:5968